Heliyon 8 (2022) e09556

Contents lists available at ScienceDirect

Heliyon

journal homepage: www.cell.com/heliyon

Research article

# Solvent effects on the crystallization and structure of ternary copper(II) coordination compounds with L-threonine and 1,10-phenanthroline☆

Darko Vušak [a], Katarina Ležaić [a], Jurica Jurec [b], Dijana Žilić [b], Biserka Prugovečki [a,*]

[a] Department of Chemistry, Faculty of Science, University of Zagreb, Horvatovac 102a, HR-10000, Zagreb, Croatia
[b] Laboratory for Magnetic Resonances, Division of Physical Chemistry, Ruđer Bošković Institute, Bijenička 54, HR-10000 Zagreb, Croatia

## GRAPHICAL ABSTRACT

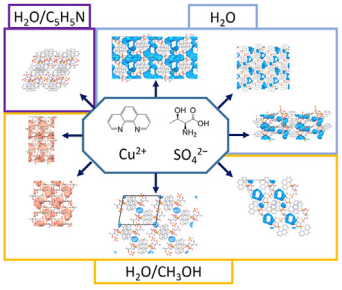


## ARTICLE INFO

*Keywords:*
Ternary coordination compounds
Solvatomorphs
Crystal structures
ESR spectra
Solution-based synthesis
Mechanochemical synthesis
Copper complexes
L-threonine
1,10-Phenanthroline

## ABSTRACT

Solution-based and solid-state reactions of copper(II) compounds, 1,10-phenanthroline and L-threonine were investigated. Eight new ternary coordination compounds were obtained: [Cu(L-Thr)($H_2O$)(phen)]$_2SO_4$•10$H_2O$ (**1a•10$H_2O$**), [Cu(L-Thr)($H_2O$)(phen)]$_2SO_4$•4.3$H_2O$ (**1a•4.3$H_2O$**), {[Cu($\mu$-L-Thr)(phen)]$_2SO_4$•3.5$H_2O$}$_n$ (**1b•3.5$H_2O$**), [Cu(L-Thr)($H_2O$)(phen)][Cu(L-Thr)($CH_3OH$)(phen)]$SO_4$•2$H_2O$•$CH_3OH$ (**1c•2$H_2O$•$CH_3OH$**), [Cu(L-Thr)($H_2O$)(phen)][Cu(L-Thr)($CH_3OH$)(phen)]$SO_4$•4$H_2O$ (**1c•4$H_2O$**), [Cu(L-Thr)($CH_3OH$)(phen)]$_2SO_4$•$H_2O$ (**1d•$H_2O$**), [Cu(L-Thr)($H_2O$)(phen)][Cu(l-Thr)($CH_3OH$)(phen)][Cu($SO_4$)(L-Thr)(phen)]$HSO_4$•$H_2O$•3$CH_3OH$ (**1e·$H_2O$·3$CH_3OH$**), [Cu(L-Thr)($H_2O$)(phen)][Cu(L-Thr)(phen)(py)]$SO_4$ (**1f**) (phen = 1,10-phenanthroline, L-Thr = L-threoninate, py = pyridine). X-ray crystal structure analysis of the prepared ternary coordination compounds revealed extensive hydrogen bonding and $\pi$-interactions that link complex species, anions and solvent molecules into 3D architectures. The water/methanol solvent molecules are found in pockets and/or channels in seven solvates. ESR spectra of different types of compounds were also investigated. In all measured compounds the unpaired electron of the copper(II) ion is located in the $d_{x2-y2}$ orbital which is in agreement with elongated square-pyramidal geometry. Compound **1a•10$H_2O$** showed substantial cytotoxic activity toward human hepatocellular carcinoma (HepG2) and acute monocytic leukaemia (THP-1) cell lines.

☆ This article is a part of the "Coordination compounds" Special issue

* Corresponding author.
*E-mail address:* biserka@chem.pmf.hr (B. Prugovečki).

https://doi.org/10.1016/j.heliyon.2022.e09556
Received 31 March 2022; Received in revised form 28 April 2022; Accepted 25 May 2022

## 1. Introduction

Investigation of ternary coordination compounds of essential metals with amino acids and heterocyclic bases have been in focus for many years. Previous studies of such coordination compounds can be divided into three main study directions: biological activity, crystal structures and porosity. Most studies of these systems include copper as an essential metal. Copper is important for the function of several enzymes and proteins (cytochrome oxidase, superoxide dismutase, ascorbate oxidase, tyrosinase). Its deficiency or overload is associated with Menkes and Wilson disease, respectively [1].

Several Cu coordination compounds with amino acids and heterocyclic ligands have been prepared and some of them have been identified as potential drugs [2, 3, 4, 5, 6, 7] or functional porous materials [8, 9, 10]. Ruiz-Azuara has invented a process to prepare ternary coordination compounds of the type $[Cu(N–N)(N–O)]NO_3$, with the N–N ligand corresponding to 4,7-diphenyl-1,10-phenanthroline and the N–O ligand preferably being one of the aminocarboxylates (glycinate, alaninate, isoleucinate, leucinate, serinate and valinate) to be used as anticancerogenic agents for treatment of cancerogenic tumors [11, 12]. Furthermore, Ruiz-Azuara *et al.* have investigated antineoplastic properties of a class of coordination compounds, called Casiopeinas® of the general formula $[Cu(N–N)(\alpha\text{-L-aminocarboxylate})]^{2+/+}$ (N–N ligands are substituted 2,2′-bipyridines or 1,10-phenanthrolines, α-L-aminocarboxylates are glycinate, alaninate, isoleucinate, leucinate, serinate or valinate). It was shown that the presence of a N–N ligand is crucial for preservation of antiproliferative activity, whereas the α-L-aminocarboxylate withdraws electrons and enhances π-interactions with adenine. Also, an aminocarboxylate as a ligand with various binding possibilities contributes to other properties such as plasticity of the coordination sphere, prevention of oxidation and biocompatibility of the metal ion environment. Some of these complexes can induce cell apoptosis *in vitro* and also exhibit excellent *in vivo* antitumor activity [13].

Since amino acids possess different side chains, their coordination compounds can create structures of higher dimensionalities (1D, 2D and 3D) through different non-covalent interactions (hydrogen bonds, π-stacking). In most of the ternary copper coordination compounds with amino acids and 1,10-phenanthroline the copper(II) atom is either five- or six-coordinated [14]. Depending on the amino acid and the presence of a heterocyclic base, different architectures can be formed and, among others, porous structures into which can be incorporated guest molecules such as solvents to produce different solvatomorphs [5, 15]. In CSD there are 98 data sets of ternary copper coordination compounds involving aminoacidates and 1,10-phenanthroline. These 98 data sets being published in 80 different articles show the lack of systematic exploration of the crystal structures and structure-property relationship of such copper(II) ternary coordination compounds. Only in two research articles different solvates of these ternary coordination compounds were investigated – monohydrate and unhydrated alaninato complexes [16] and six serinato solvates involving water and/or methanol [5]. Both described alaninato compounds are coordination polymers, where carboxylic group acts as bridge between two copper(II) atoms. In serinato compounds, all six compounds contain monomeric complex cations of general formula $[Cu(ser)(L)(phen)]^+$ (ser = L-serinato; L = $H_2O$ or $CH_3OH$; phen = 1, 10-phenanthroline). Three of those compounds contain only water as solvent, two of them contain only methanol, while one compound contains mixture of water and methanol molecules (coordinated and crystallization molecules).

In the early papers published in the 1980s coordination of the copper atom was the main concern of researchers [17, 18, 19], while in later papers intermolecular interactions were explored [20, 21]. In the recent years, as mentioned earlier, such ternary coordination compounds are mostly investigated for their antiproliferative activity [3, 13, 22, 23]. In contrast to solid-state, these complexes are well explored in solution. Binding modes at different pH-values of ternary coordination compounds were investigated with different amino acids and heterocyclic bases, including L-threonine and 1,10-phenanthroline [24, 25]. It was shown that ternary coordination species $[Cu(aa)(N–N)]^+$ (aa = aminoacidate; N–N = 2,2′-bipyridine or 1,10-phenanthroline) are more stable than either $[Cu(aa)_2]$ or $[Cu(N–N)_2]^{2+}$ binary compounds [25, 26, 27, 28].

As a part of our ongoing research on ternary copper(II) coordination compounds with amino acids and heterocyclic bases [5, 29, 30, 31], in this work we explored the versatility of intermolecular interactions in copper ternary coordination compounds with L-threonine and 1,10-phenanthroline for the purpose of crystal engineering and investigation of structure-property relationships, such as magnetic property (ESR spectroscopy) or biological activity. We have performed the reactions of copper (II) compounds with L-threonine and 1,10-phenanthroline by solution methods and solid-state reactions. These two ligands were chosen having in mind a polar ligand and a nonpolar ligand, and their ability to form different types of intermolecular contacts. The effects of solvent (water, methanol, pyridine (py) or their binary mixtures) on crystallization and crystal structures was investigated. The following new compounds were obtained: $[Cu(L\text{-Thr})(H_2O)(phen)]_2SO_4•10H_2O$ (**1a•10H$_2$O**), $[Cu(L\text{-Thr})(H_2O)(phen)]_2SO_4•4.3H_2O$ (**1a•4.3H$_2$O**), $\{[Cu(\mu\text{-L-Thr})(phen)]_2SO_4•3.5H_2O\}_n$ (**1b•3.5H$_2$O**), $[Cu(L\text{-Thr})(H_2O)(phen)][Cu(L\text{-Thr})(CH_3OH)(phen)]SO_4•2H_2O•CH_3OH$ (**1c•2H$_2$O•CH$_3$OH**), $[Cu(L\text{-Thr})(H_2O)(phen)][Cu(L\text{-Thr})(CH_3OH)(phen)]SO_4•4H_2O$ (**1c•4H$_2$O**), $[Cu(L\text{-Thr})(CH_3OH)(phen)]_2SO_4•H_2O$ (**1d•H$_2$O**), $[Cu(L\text{-Thr})(H_2O)(phen)][Cu(L\text{-Thr})(CH_3OH)(phen)][Cu(SO_4)(L\text{-Thr})(phen)]HSO_4•H_2O•3CH_3OH$ (**1e·H$_2$O·3CH$_3$OH**), $[Cu(L\text{-Thr})(H_2O)(phen)][Cu(L\text{-Thr})(phen)(py)]SO_4$ (**1f**).

## 2. Materials and methods

Copper(II) sulfate pentahydrate (Gram-Mol), anhydrous copper (II) sulfate (Acros), 1,10-phenanthroline monohydrate (Merck), L-threonine (Fischer Scientific), methanol (Alkaloid), DMEM/F12 medium (Sigma), FBS (Sigma), DMSO (Sigma) and staurosporine (Sigma) were obtained from commercial sources and used without further purification. Copper(II) hydroxide was prepared by the method of Agte [32, 33]. Copper(II) sulfate trihydrate was prepared by heating copper(II) sulfate pentahydrate to 100 °C and copper(II) sulfate monohydrate by heating copper(II) sulfate pentahydrate to 150 °C. Anhydrous 1,10-phenanthroline was prepared by heating 1,10-phenanthroline monohydrate to 130 °C. Attenuated total reflectance infrared (ATR-IR) spectra were measured on a Thermo Scientific™ Nicolet™ iS50 FTIR Spectrometer equipped with an ATR module in the spectral range 4000–400 $cm^{-1}$ with a resolution of 4 $cm^{-1}$. Powder X-ray diffraction (PXRD) was performed on a Malvern Panalytical Aeris diffractometer in a Bragg-Brentano geometry with Cu$K_\alpha$ radiation ($\lambda$ = 1.54184 Å) at room temperature. The samples were contained on a silicon holder and the diffractograms were measured in 2$\theta$ range 5–40° with a step size of 0.022° and 15.0 s of measurement time per step. PXRD data were analyzed using HighScore Plus program [34]. Mechanochemical syntheses were performed on a Retch MM200 grinder operating at frequency of 25 Hz for 15 min. Teflon jars (volume 14 mL) and stainless steel balls (diameter 8 mm) were used for grinding.

### 2.1. Solution-based syntheses

#### 2.1.1. Synthesis and crystallization of $[Cu(L\text{-Thr})(H_2O)(phen)]_2SO_4·10H_2O$ (1a·10H$_2$O) and $[Cu(L\text{-Thr})(H_2O)(phen)]_2SO_4·4.3H_2O$ (1a·4.3H$_2$O)

Copper(II) sulphate pentahydrate (64.1 mg, 0.25 mmol), copper(II) hydroxide (25.5 mg, 0.25 mmol), 1,10-phenanthroline monohydrate (101.1 mg, 0.5 mmol) and L-threonine (60.2 mg, 0.5 mmol) were dissolved in water (10 mL). Solution was heated at 100 °C for 45 min. The solution was filtered and slowly evaporated for a week. Eventually, dark blue needles of either **1a·10H$_2$O** and/or **1a·4.3H$_2$O** crystallized. Crystals of **1a·10H$_2$O** were suitable for single-crystal X-ray diffraction analysis.

Crystals of **1a·4.3H$_2$O** diffracted poorly so synchrotron radiation was used for data collection. Both crystals of **1a·10H$_2$O** and **1a·4.3H$_2$O** decompose when taken out of the solution. IR (ATR) for **1a·10H$_2$O**: $\tilde{\nu}$ /cm$^{-1}$ = 3600–2900 (m), 3341 (s), 3255 (s), 3120 (s), 3060 (m), 2976 (m), 2935(m), 2806 (w), 1658 (s), 1603 (s), 1519 (m), 1494 (w), 1430 (m), 1402 (m), 1367 (m), 1345 (w), 1298 (w), 1262 (w), 1224 (w), 1185 (m), 1142 (m), 1099 (m), 1059 (s), 1035 (s), 1005 (m), 976 (m), 911 (m), 874 (m), 856 (s), 813 (w), 783 (w), 736 (w), 722 (s), 681 (w), 645 (w), 605 (w), 576(w), 556 (w), 474 (w), 428 (m).

#### 2.1.2. Synthesis and crystallization of [Cu(L-Thr)(H$_2$O)(phen)]$_2$SO$_4$·10H$_2$O (1a·10H$_2$O)

Copper(II) sulphate pentahydrate (64.6 mg, 0.25 mmol), copper(II) hydroxide (25.2 mg, 0.25 mmol), 1,10-phenanthroline monohydrate (100.3 mg, 0.5 mmol) and L-threonine (61.3 mg, 0.5 mmol) were dissolved in methanol/water mixture (10 mL; $v/v$ = 7:3 or 1:9) and heated for 45 min at 80 °C. The dark blue solution was filtered and after few days dark blue needles of **1a·10H$_2$O** were formed. Crystals were suitable for single-crystal X-ray diffraction analysis.

#### 2.1.3. Synthesis and crystallization of [Cu(L-Thr)(H$_2$O)(phen)]$_2$SO$_4$·10H$_2$O (1a·10H$_2$O), [Cu(L-Thr)(H$_2$O)(phen)][Cu(L-Thr)(CH$_3$OH)(phen)]SO$_4$•2H$_2$O•CH$_3$OH (1c•2H$_2$O•CH$_3$OH) and [Cu(L-Thr)(phen)(CH$_3$OH)]$_2$SO$_4$·H$_2$O (1d·H$_2$O)

Copper(II) sulphate pentahydrate (64.1 mg, 0.25 mmol), copper(II) hydroxide (24.7 mg, 0.25 mmol), 1,10-phenanthroline monohydrate (99.2 mg, 0.5 mmol) and L-threonine (59.3 mg, 0.5 mmol) were dissolved in methanol (10 mL). The solution was heated at 80 °C for 45 min and filtered. Dark blue solution was left to evaporate and after few days dark blue needles (**1a·10H$_2$O**) and/or prisms (**1c•2H$_2$O•CH$_3$OH** and/or **1d·H$_2$O**) suitable for single-crystal X-ray analysis were formed. Crystals of **1c•2H$_2$O•CH$_3$OH** slowly decompose outside of solution while those of **1d·H$_2$O** are stable at room temperature. IR (ATR) for **1c•2H$_2$O•CH$_3$OH**: $\tilde{\nu}$ /cm$^{-1}$ = 3600–2900 (m), 3206 (s), 3114 (s), 2978 (m), 2935(m), 2906 (m), 2832 (m), 1630 (s), 1610 (s), 1518 (m), 1496 (w), 1429 (m), 1386 (m), 1361 (m), 1347 (m), 1260 (w), 1228 (w), 1196 (m), 1140 (m), 1084 (m), 1054 (s), 1044 (s), 1027 (s), 1002 (s), 968 (m), 902 (m), 867 (m), 853 (s), 808 (w), 783 (w), 741 (m), 722 (s), 686 (w), 650 (w), 611 (w), 556 (s), 490 (w), 466 (w), 431 (m).

#### 2.1.4. Synthesis and crystallization of [Cu(L-Thr)(H$_2$O)(phen)][Cu(L-Thr)(CH$_3$OH)(phen)]SO$_4$•4H$_2$O (1c•4H$_2$O) and [Cu(L-Thr)(H$_2$O)(phen)][Cu(L-Thr)(CH$_3$OH)(phen)][Cu(SO$_4$)(L-Thr)(phen)]HSO$_4$·H$_2$O·3CH$_3$OH (1e·H$_2$O·3CH$_3$OH)

Copper(II) sulphate monohydrate (46.8 mg, 0.25 mmol), copper(II) hydroxide (24.9 mg, 0.25 mmol), anhydrous 1,10-phenanthroline (90.9 mg, 0.5 mmol), and L-threonine (62.3 mg, 0.5 mmol) were dissolved in methanol (10 mL). The solution was heated at 80 °C for 45 min, filtered and left to evaporate. Eventually, dark blue prisms (**1c•4H$_2$O**) and/or needles (**1e·H$_2$O·3CH$_3$OH**) formed after a few weeks. Crystals of **1e·H$_2$O·3CH$_3$OH** are highly unstable outside solution and decompose in few seconds. Crystals of **1c•4H$_2$O** were suitable for single-crystal X-ray diffraction, while crystals of **1e·H$_2$O·3CH$_3$OH** diffracted poorly and were analysed by synchrotron irradiation.

#### 2.1.5. Synthesis and crystallization of [Cu(L-Thr)(phen)(CH$_3$OH)]$_2$SO$_4$·H$_2$O (1d·H$_2$O) and [Cu(L-Thr)(H$_2$O)(phen)][Cu(L-Thr)(CH$_3$OH)(phen)][Cu(SO$_4$)(L-Thr)(phen)]HSO$_4$•H$_2$O•3CH$_3$OH (1e·H$_2$O·3CH$_3$OH)

Anhydrous copper(II) sulphate (40.0 mg, 0.25 mmol), copper(II) hydroxide (24.3 mg, 0.25 mmol), anhydrous 1,10-phenanthroline (90.1 mg, 0.5 mmol) and L-threonine (60.3 mg, 0.5 mmol) were dissolved in methanol (10 mL). The solution was heated at 80 °C for 45 min, filtered and left to evaporate. After a few days blue prisms (**1d·H$_2$O**), needles (**1e·H$_2$O·3CH$_3$OH**) and/or light blue prisms ([Cu(SO$_4$)(phen)$_2$]·CH$_3$OH (CSD refcode MUNHIO [35]) were formed.

#### 2.1.6. Synthesis and crystallization of {[Cu(μ-L-Thr)(phen)]$_2$SO$_4$·3.5H$_2$O}$_n$ (1b·3.5H$_2$O)

Copper(II) sulphate pentahydrate (66.0 mg, 0.25 mmol), copper(II) hydroxide (24.5 mg, 0.25 mmol), 1,10-phenanthroline monohydrate (101.2 mg, 0.5 mmol), L-threonine (61.5 mg, 0.5 mmol) were dissolved in a water/pyridine mixture (10 mL; $v/v$ = 1:9) and heated at 80 °C for 45 min, filtered and left to evaporate. After a few days blue needles of **1b·3.5H$_2$O** were formed. Crystals of **1b·3.5H$_2$O** are unstable outside of solution, but were suitable for single-crystal X-ray diffraction analysis. IR (ATR) for **1b·3.5H$_2$O**: $\tilde{\nu}$ /cm$^{-1}$ = 3600–2900 (m), 3294 (m), 3089 (s), 3062 (m), 3044 (m), 3023 (m), 2972 (w), 2933 (m), 2830 (w), 1623 (s), 1603 (s), 1519 (m), 1492 (m), 1448 (m), 1430 (m), 1400 (m), 1387 (m), 1349 (w), 1315 (w), 1267 (w), 1260 (w), 1224 (w), 1162 (m), 1144 (m), 1072 (s), 1050 (s), 1043 (s), 1013 (m), 903 (m), 873 (m), 851 (s), 807 (w), 779 (m), 761 (m), 739 (m), 719 sw), 700 (s), 637 (w), 616 (w), 599 (m), 558 (w), 540 (w), 534 (w), 523 (w), 510 (w), 500 (w), 490 (w), 482 (w), 466 (w), 446 (m), 430 (m), 416 (m).

#### 2.1.7. Synthesis and crystallization of [Cu(L-Thr)(phen)(CH$_3$OH)]$_2$SO$_4$·2H$_2$O (1d·H$_2$O)

Copper(II) sulphate pentahydrate (66.1 mg, 0.25 mmol), copper(II) hydroxide (24.8 mg, 0.25 mmol), 1,10-phenanthroline monohydrate (99.5 mg, 0.5 mmol), L-threonine (62.3 mg, 0.5 mmol) were dissolved in methanol/pyridine mixture (10 mL; $v/v$ = 9:1) and heated at 80 °C for 45 min, filtered and left to evaporate. After a few weeks blue prisms of **1d·H$_2$O** were formed.

#### 2.1.8. Synthesis and crystallization of {[Cu(μ-L-Thr)(phen)]$_2$SO$_4$·3.5H$_2$O}$_n$ (1b·3.5H$_2$O) and [Cu(L-Thr)(phen)(CH$_3$OH)]$_2$SO$_4$·2H$_2$O (1d·H$_2$O)

Copper(II) sulphate pentahydrate (63.0 mg, 0.25 mmol), copper(II) hydroxide (24.5 mg, 0.25 mmol), 1,10-phenanthroline monohydrate (99.8 mg, 0.5 mmol), and L-threonine (59.6 mg, 0.5 mmol) were dissolved in methanol/pyridine mixture (10 mL; $v/v$ = 7:3) and heated at 80 °C for 45 min, filtered and left to evaporate. After a few days blue needles of **1b·3.5H$_2$O** and/or prisms of **1d·H$_2$O** were formed.

#### 2.1.9. Synthesis and crystallization of [Cu(L-Thr)(H$_2$O)(phen)][Cu(L-Thr)(phen)(py)]SO$_4$ (1f)

Copper(II) sulphate pentahydrate (63–64 mg, 0.25 mmol), copper(II) hydroxide (24 mg, 0.25 mmol), 1,10-phenanthroline monohydrate (100–106 mg, 0.5 mmol) and L-threonine (62–66 mg, 0.5 mmol) were dissolved in a methanol/pyridine mixture (10 mL; $v/v$ = 3:7 or 1:9) and heated at 80 °C for 45 min, filtered and left to evaporate. After several weeks few prisms of **1f** were formed. IR (ATR) for **1f**: $\tilde{\nu}$ /cm$^{-1}$ = 3550–2900 (m), 3226 (s), 3154 (m), 3058 (s), 3008 (m), 2965 (m), 2930 (m), 2873 (w), 1630 (s), 1600 (s), 1586 (s), 1520 (m), 1492 (w), 1432 (m), 1416 (w), 1371 (m), 1348 (m), 1325 (m), 1277 (w), 1221 (m), 1145 (m), 1095 (m), 1064 (m), 1032 (s), 1009 (m), 958 (m), 938 (m), 921 (w), 909 (w), 873 (m), 863 (s), 847 (s), 780 (m), 761 (m), 739 (m), 722 (s), 706 (s), 648 (m), 623 (w), 600 (s), 582 (m), 562 (w), 509 (w), 499 (w), 490 (w), 460 (w), 445 (m), 429 (m), 417 (m), 408 (m).

### 2.2. Mechanochemical syntheses

#### 2.2.1. Synthesis of [Cu(L-Thr)(H$_2$O)(phen)]$_2$SO$_4$·10H$_2$O (1a·10H$_2$O)

Copper(II) sulphate pentahydrate (62.5 mg, 0.25 mmol), copper(II) hydroxide (24.4 mg, 0.25 mmol), anhydrous 1,10-phenanthroline (90.2 mg, 0.5 mmol) and L-threonine (59.5 mg, 0.5 mmol) were mixed in a Teflon jar ($V$ = 14 mL) and 24 μL of water was added ($\eta$ = 0.1 μL mg$^{-1}$) [36]. Grinding was performed using one steel ball (8 mm) at a vibration frequency 25 Hz for 15 min. The product was analysed by powder X-ray diffraction. Powder diffraction pattern was consistent with powder pattern calculated from crystal structure of **1a·10H$_2$O** (Fig. S1 in Supplementary information). Another PXRD experiments were performed on

the same sample after 2 and 5 min and it was confirmed that the decomposition of compound began (Fig. S1 in Supplementary information).

#### 2.2.2. Synthesis of $[Cu(L\text{-}Thr)(H_2O)(phen)]_2SO_4{\cdot}10H_2O$ (**1a·10H$_2$O**) and $[Cu(L\text{-}Thr)(H_2O)(phen)][Cu(L\text{-}Thr)(CH_3OH)(phen)]SO_4{\cdot}2H_2O{\cdot}CH_3OH$ (**1c·2H$_2$O·CH$_3$OH**)

Copper(II) sulphate pentahydrate (62.4 mg, 0.25 mmol), copper(II) hydroxide (24.7 mg, 0.25 mmol), anhydrous 1,10-phenanthroline (90.1 mg, 0.5 mmol) and L-threonine (59.9 mg, 0.5 mmol) were mixed in a Teflon jar ($V$ = 14 mL) and 47 μL of methanol was added ($\eta$ = 0.2 μL mg$^{-1}$). Grinding was perfomed using one steel ball (8 mm) at vibration frequency 25 Hz for 15 min. The product was analysed by powder X-ray diffraction. The powder diffraction pattern was consistent with the powder pattern calculated from crystal structures of **1a·10H$_2$O** and **1c·2H$_2$O·CH$_3$OH** (Fig. S1 in Supplementary information).

#### 2.2.3. Synthesis of $[Cu(L\text{-}Thr)(H_2O)(phen)][Cu(L\text{-}Thr)(CH_3OH)(phen)]SO_4{\cdot}2H_2O{\cdot}CH_3OH$ (**1c·2H$_2$O·CH$_3$OH**)

Copper(II) sulphate trihydrate (53.5 mg, 0.25 mmol), copper(II) hydroxide (24.3 mg, 0.25 mmol), anhydrous 1,10-phenanthroline (90.5 mg, 0.5 mmol) and L-threonine (59.5 mg, 0.5 mmol) were mixed in a Teflon jar ($V$ = 14 mL) and 46 μL of methanol was added ($\eta$ = 0.2 μL mg$^{-1}$). Grinding was perfomed using one steel ball (8 mm) at vibration frequency 25 Hz for 15 min. The product was analysed by powder X-ray diffraction. The powder diffraction pattern was consistent with the powder pattern calculated from crystal structure of **1c·2H$_2$O·CH$_3$OH** (Fig. S1 in Supplementary information).

#### 2.2.4. Synthesis of $[Cu(L\text{-}Thr)(CH_3OH)(phen)]_2SO_4{\cdot}H_2O$ (**1d·H$_2$O**)

Anhydrous copper(II) sulphate (39.9 mg, 0.5 mmol), copper(II) hydroxide (24.7 mg, 0.25 mmol), anhydrous 1,10-phenanthroline (90.1 mg, 0.5 mmol) and L-threonine (59.5 mg, 0.5 mmol) were mixed in a Teflon jar ($V$ = 14 mL) and 43 μL of methanol was added ($\eta$ = 0.2 μL mg$^{-1}$). Grinding was perfomed using one steel ball (8 mm) at vibration frequency 25 Hz for 15 min. The product was analysed by powder X-ray diffraction. Most diffraction maxima were consistent with the powder pattern calculated from the crystal structure of **1d·H$_2$O**, but a small amount of unknown phase was also detected (Fig. S1 in Supplementary information).

### 2.3. Single-crystal X-ray diffraction

Single-crystal X-ray diffraction data of **1a•10H$_2$O**, **1b•3.5H$_2$O**, **1c•2H$_2$O•CH$_3$OH**, **1c•4H$_2$O** and **1f** were measured on a Rigaku XtaLAB Synergy diffractometer using Cu$K_\alpha$ radiation ($\lambda$ = 1.54184 Å) with HyPix6000HE detector at 170 (**1b•3.5H$_2$O**, **1c•2H$_2$O•CH$_3$OH**, **1c•4H$_2$O** and **1f**) or 180 K (**1a•10H$_2$O**). Diffraction data of **1d•H$_2$O** were collected on an Oxford Diffraction Xcallibur3 CCD diffractometer using Mo$K_\alpha$ radiation ($\lambda$ = 0.71073 Å) at room temperature. X-ray diffraction data of **1a•4.3H$_2$O** and **1e·H$_2$O·3CH$_3$OH** were collected at Elettra Sincrotrone Trieste using synchrotron radiation ($\lambda$ = 0.70000 Å) at XRD1 beamline equipped with Dectris Pilatus 2M detector at 100 K. Data reduction for all data sets was performed using the CrysAlis software package [37]. All crystal structures except **1f** were solved by SHELXS [38] and **1f** was solved by SHELXT [39] program. Full-matrix least-squares refinements based on $F^2$ against all reflections were carried out by a SHELXL-2017/1 program [40]. Structures were visualized using the Mercury program [41]. Geometrical parameters were calculated with PLATON [42]. All nonhydrogen atoms were refined anisotropically. Most of the hydrogen atoms were refined at calculated positions. Hydrogen atoms belonging to the water or methanol molecules and hydrogensulfate ions were found in the Fourier difference maps and restrained to positions according to the idealized geometry of the respective group. In **1a•4.3H$_2$O** hydrogen atoms belonging to water molecules were constrained to positions found in the Fourier difference map according to the idealized geometry. One of the symmetrically independent L-threoninate residue in **1a•4.3H$_2$O** is disordered over two sites with occupancies of 0.52 and 0.48. In the part with the higher occupancy factor one water molecule is also present (with the same occupancy factor), while in the other part there is no additional water molecule, so the average number of crystallization water molecules per formula unit is 4.3. In **1b•3.5H$_2$O** one of the symmetrically independent sulfate ion is disordered over two positions around one of the S–O axis, so that three oxygen atoms are split in two parts with individual occupancy factors 0.67 and 0.33. After visualization of the crystal structure of **1a•10H$_2$O** it was noticed that two unusually large voids are present in the structure (volume of each void ≈20 Å$^3$, calculated with PLATON), however, there is no significant residual electron density inside voids.

### 2.4. ESR spectroscopy

The ESR measurements were performed on a Bruker Elexsys 580 FT/CW spectrometer from the room down to the liquid nitrogen temperature. The microwave frequency was around 9.7 GHz with the magnetic field modulation amplitude of 0.5 mT and modulation frequency of 100 kHz. The investigated compounds **1a·10H$_2$O** and **1b•3.5H$_2$O** were unstable outside of solution so the samples were kept in respective mother liquors till measurements.

### 2.5. In vitro cytotoxic activity

Cytotoxicity experiments were performed at the School of Medicine, University of Zagreb. Since all prepared compounds contain similar complex species which are biologically active, we chose **1a·10H$_2$O** as the representative compound. All prepared compounds are highly soluble in water and moderately soluble in methanol and DMSO. The *in vivo* cytotoxicity of the **1a•10H$_2$O** was assessed on the hepatocellular carcinoma (HepG2, ATCC HB−8065) and human acute monocytic leukaemia (THP-1, ATCC TIB−202) cell lines. CellTiter 96® AQueous One Solution Cell Proliferation Assay (MTS) was used. It is a tetrazolium-based cell viability assay that measures the metabolic capacity of cells in culture [43]. Serial dilutions of the tested compound in 96-well microtiter plates were prepared in 100–0.05 μM concentration range in an appropriate cell medium (50 μL). Cells were added to plates in an appropriate number per well (50 μL). Control wells consisted of media only (blank) or cells with 1% DMSO added (control). Plates were incubated overnight at 37 °C in a 5% $CO_2$ atmosphere. For determining inhibition of cellular proliferation or inducement of cytotoxic effect CellTiter 96 Aqueous One Solution Cell Proliferation Assay (Promega, G3580) was used. 10 μL of MTS reagent was dispensed per well. Plates were incubated for 2 h at 37 °C in a 5% $CO_2$ atmosphere and the absorbance was recorded at 490 nm using a 96-well Spectramax i3x plate reader. Results were analyzed in GraphPad Prism software.

## 3. Results and discussion

### 3.1. Synthesis and crystallization

Overview of the solution-based synthetic procedures of all eight coordination compounds is given in Scheme 1. All monomeric compounds except **1e·H$_2$O·3CH$_3$OH** contain two complex cations, $[Cu(L\text{-}Thr)(L)(phen)]^+$ (L = $H_2O$, $CH_3OH$ and/or py), and a sulfate counterion while **1e·H$_2$O·3CH$_3$OH** contains three complex units, $[Cu(L\text{-}Thr)(H_2O)(phen)]^+$, $[Cu(L\text{-}Thr)(CH_3OH)(phen)]^+$ and $[Cu(SO_4)(L\text{-}Thr)(phen)]^-$ and a hydrogen sulfate counterion. Compound **1b·3.5H$_2$O** contains polymeric chains $\{[Cu(\mu\text{-}L\text{-}Thr)(phen)]^+\}_n$ and sulfate counter ions. As seen in Scheme 1, many synthetic conditions yielded two or three different products. If fully hydrated reactants (copper(II) sulfate pentahydrate, 1,10-phenanthroline monohydrate) in pure water or high ratio of water is used, **1a·10H$_2$O** crystallizes in most cases, and in some cases **1a·4.3H$_2$O** or their mixture. If fully hydrated reactants and pure

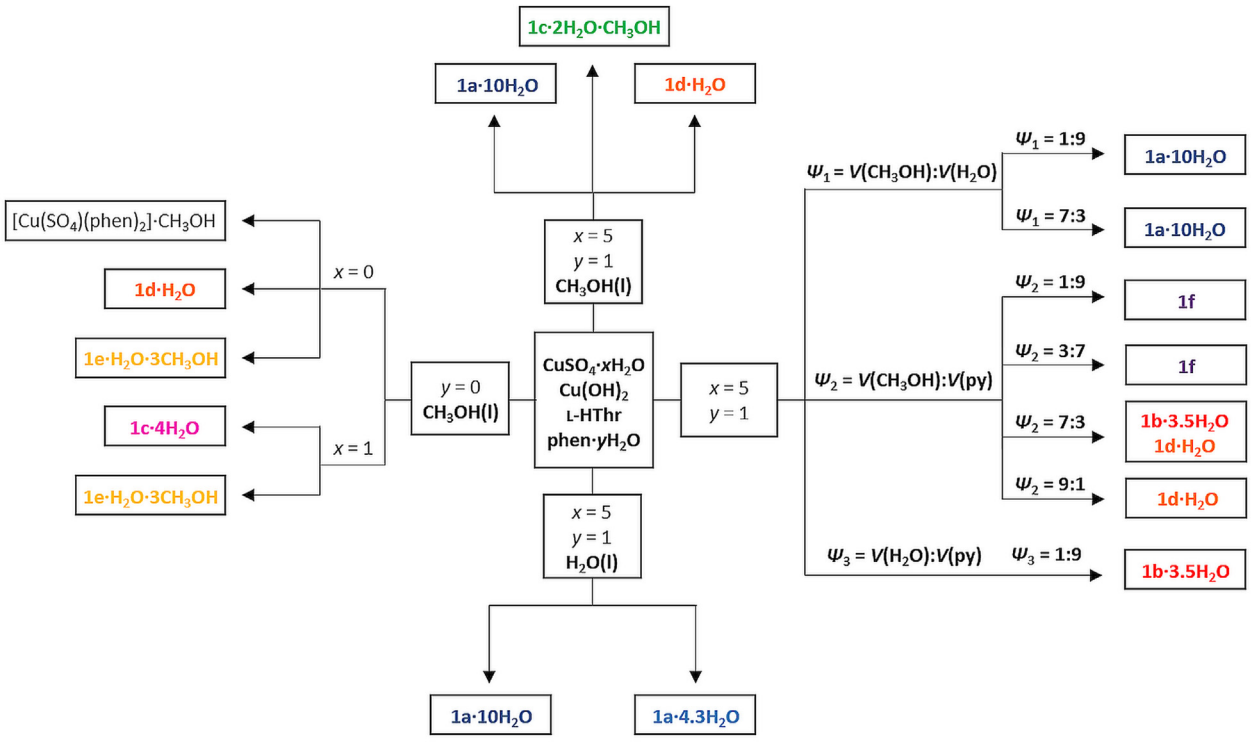


**1a·10H$_2$O** = [Cu(L-Thr)(H$_2$O)(phen)]$_2$SO$_4$·10H$_2$O
**1a·4.3H$_2$O** = [Cu(L-Thr)(H$_2$O)(phen)]$_2$SO$_4$·4.3H$_2$O
**1b·3.5H$_2$O** = {[Cu($\mu$-L-Thr)(phen)]$_2$SO$_4$·3.5H$_2$O}$_n$
**1c·4H$_2$O** = [Cu(L-Thr)(H$_2$O)(phen)][Cu(L-Thr)(CH$_3$OH)(phen)]SO$_4$·4H$_2$O
**1c·2H$_2$O·CH$_3$OH** = [Cu(L-Thr)(H$_2$O)(phen)][Cu(L-Thr)(CH$_3$OH)(phen)]SO$_4$·2H$_2$O·CH$_3$OH
**1d·H$_2$O** = [Cu(L-Thr)(phen)(CH$_3$OH)]$_2$SO$_4$·H$_2$O
**1e·H$_2$O·3CH$_3$OH** = [Cu(L-Thr)(H$_2$O)(phen)][Cu(L-Thr)(CH$_3$OH)(phen)][Cu(SO$_4$)(L-Thr)(phen)]HSO$_4$·H$_2$O·3CH$_3$OH
**1f** = [Cu(L-Thr)(H$_2$O)(phen)][Cu(L-Thr)(phen)(py)]SO$_4$
[Cu(SO$_4$)(phen)$_2$]·CH$_3$OH (CSD refcode MUNHIO)

**Scheme 1.** Solution-based syntheses of all eight copper(II) coordination compounds.

methanol as solvent are used three different products crystallized: **1a·10H$_2$O**, **1c·2H$_2$O·CH$_3$OH** and/or **1d·H$_2$O**. If less hydrated reactants (anhydrous or monohydrate of copper(II) sulfate, anhydrous 1,10-phenanthroline) and pure methanol were used **1c·4H$_2$O**, **1d·H$_2$O** and/or **1e·H$_2$O·3CH$_3$OH** crystallized from the solution. If we look at the formula units of **1c·4H$_2$O**, **1c·2H$_2$O·CH$_3$OH**, **1d·H$_2$O** and **1e·H$_2$O·3CH$_3$OH** it is seen that all these compounds contain both water and methanol molecules (coordinated and/or as crystallization molecules) so it is possible that at high methanol to water ratio, there is small difference in their stability and there is a possibility for any of them to crystallize. Small variances of conditions, such as room temperature, evaporation rate or size and shape of the crystallization dish, may influence the final crystal product. **1b•3.5H$_2$O** crystallized from the water/pyridine mixture ($v/v$ = 1:9). The same product crystallizes from the methanol/pyridine solution ($v/v$ = 7:3), but in a mixture with **1d·H$_2$O**. It seems pyridine has an effect as a tailor-made additive on the formation of polymeric **1b•3.5H$_2$O**. At higher pyridine to methanol ratio **1f** crystallizes but with an extremely low yield, due to low solubility of reactants. Although in some of the synthetic conditions there is a very low water content, water is present in all products (coordinated and/or as crystallization molecules). The ability of water molecules to act as donors and acceptors of hydrogen bonds may be crucial for the stability of crystal structures in these ternary coordination compounds.

Similar to the solution-based syntheses, small differences in water content influenced the final product of mechanochemical syntheses so we tried to use different hydrates of copper(II) sulfate and 1,10-phenanthroline. Three compounds were obtained from mechanochemical syntheses: **1a·10H$_2$O**, **1c·2H$_2$O·CH$_3$OH** and **1d·H$_2$O**. Compound **1a·10H$_2$O** was obtained when copper(II) sulphate pentahydrate, copper(II) hydroxide, anhydrous 1,10-phenanthroline and small amount of water were used for LAG synthesis. The same product, but in a mixture with **1c·2H$_2$O·CH$_3$OH**, was obtained when water was replaced by a small amount of methanol. If copper(II) sulfate pentahydrate was replaced by copper(II) sulfate trihydrate and small amount of methanol was used for LAG synthesis, pure **1c·2H$_2$O·CH$_3$OH** was obtained. When anhydrous reactants (copper(II) sulfate and 1,10-phenanthroline) and small amount of methanol were used **1d·H$_2$O** was obtained, but a small amount of an unknown phase was also present.

### 3.2. Infrared spectroscopy

IR (ATR) spectra were measured for **1a•10H$_2$O**, **1b•3.5H$_2$O**, **1c•2H$_2$O•CH$_3$OH** and **1f**. IR spectra of all analysed compounds are very similar to each other due to similarity in the structure and coordination of the ligands. A broad band in the range 3600–2900 cm$^{-1}$ (3550–2900 cm$^{-1}$ for **1f**) corresponding to O–H stretching suggests extensive hydrogen bonding in the crystal structures. Since there are two or more symmetrically independent L-threoninate ligands in all compounds, several bands corresponding to asymmetric stretching of the carboxylate groups are overlapped. In all cases, at least two bands can be

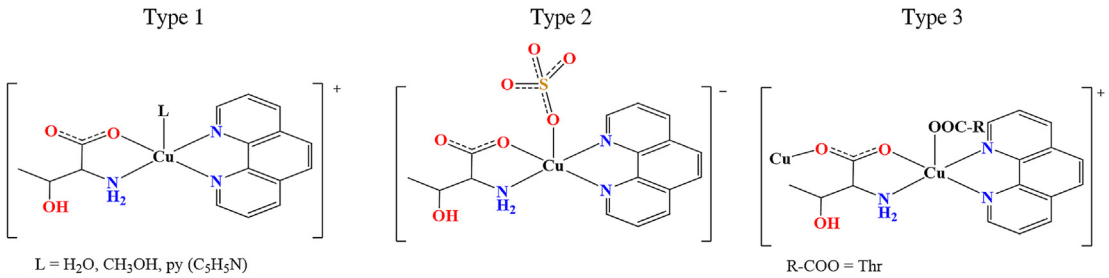


**Figure 1.** Three types of complex species based on copper(II) coordination in the apical position.

distinguished one at higher wavenumbers in the range 1658–1623 $cm^{-1}$ (uncoordinated or bridging oxygen atom) and one at lower wavenumbers in the range 1610–1600 $cm^{-1}$ (coordinated oxygen atom).

### 3.3. Crystal structures

All compounds crystallize in noncentrosymmetric space groups in either monoclinic or triclinic crystal system. Crystallographic data are given in Tables S1 and S2 in Supplementary information. The asymmetric units of **1a•10$H_2O$**, **1a•4.3$H_2O$**, **1b•3.5$H_2O$**, **1c•2$H_2O$•$CH_3OH$**, **1c•4$H_2O$**, **1d•$H_2O$**, **1e·$H_2O$·3$CH_3OH$** and **1f** are shown in Figs. S2 and S3 in Supplementary information.

#### 3.3.1. Coordination of copper(II) ion

All compounds are composed of complex species of three different types (type 1, type 2 and/or type 3), considering a molecule or ion coordinated to copper(II) ion in the apical position (Figure 1), with sulfate or hydrogensulfate counterions (Fig. S2 and S3 in Supplementary information).

In complex cations of type 1, solvent molecule (water, methanol or pyridine) is coordinated in the apical position, forming complex cations $[Cu(L\text{-Thr})(L)(phen)]^+$ (L = $H_2O$, $CH_3OH$ or py). All compounds except **1b·3.5$H_2O$** contain type 1 complex cations. We have obtained two different hydrates with two cations of type 1 with apically coordinated water molecule, **1a•10$H_2O$** and **1a•4.3$H_2O$**; one hydrate with two cations of type 1 with apically coordinated methanol molecule, **1d•$H_2O$**; two different solvates with one cation of type 1 with apically coordinated water and one with a methanol molecule, **1c•2$H_2O$•$CH_3OH$** and **1c•4$H_2O$**; as well as compound **1f** with one cation of type 1 with apically coordinated water and one with coordinated pyridine molecule. Type 2 complex anion has coordinated sulfate anion in the apical position forming complex anion $[Cu(SO_4)(L\text{-Thr})(phen)]^-$. Only compound **1e·$H_2O$·3$CH_3OH$** contains type 2 complex anion together with two complex cations of type 1 (one cation with an apically coordinated water and one with a methanol molecule) (Figure 2). Complex unit of type 3 is quite different since it contains carboxylate of adjacent complex cation coordinated to copper(II) ion in the apical position forming a polymeric chain $\{[Cu(\mu\text{-L-Thr})(phen)]^+\}_n$. **1b·3.5$H_2O$** is the only compound containing a type 3 complex unit.

All eight ternary coordination compounds contain copper(II) square-pyramidal pentacoordinated complex species, with elongated apical Cu–X bond (X = O or N), due to the Jahn-Teller effect. In all types of the investigated compounds, 1,10-phenanthroline and L-threoninate are

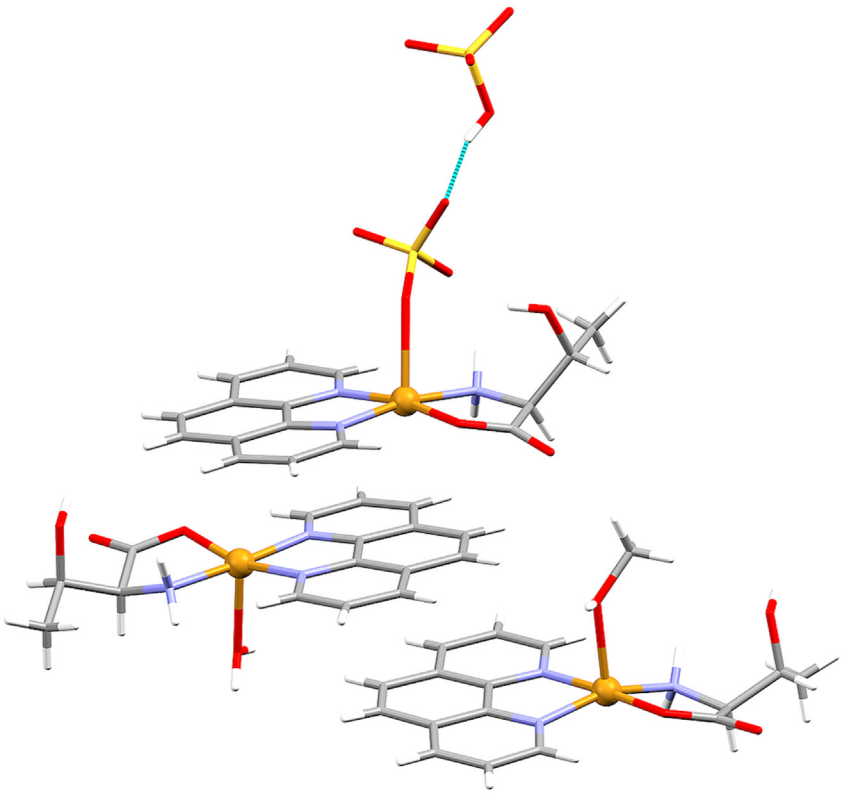

**Figure 2.** Type 1 ($[Cu(L\text{-Thr})(H_2O)(phen)]^+$ and $[Cu(L\text{-Thr})(CH_3OH)(phen)]^+$) and type 2 ($[Cu(SO_4)(L\text{-Thr})(phen)]^-$) complex species in **1e·$H_2O$·3$CH_3OH$**. Hydrogen bond between hydrogen sulfate ion and coordinated sulfate is presented with blue dotted line.

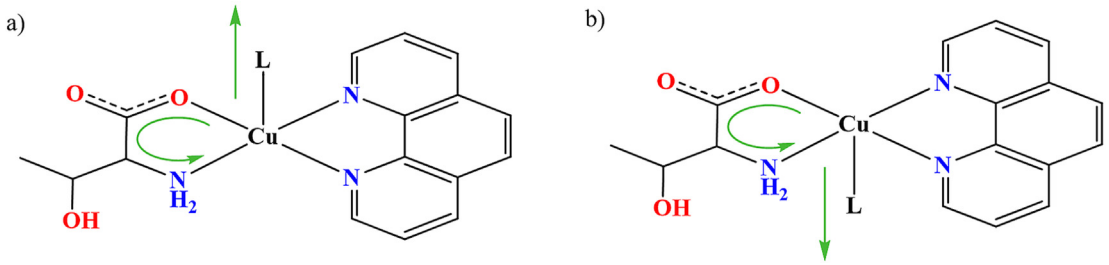


**Figure 3.** Right-hand rule for defining a) "up", ↑ and b) "down", ↓ optical isomers in ternary copper(II) coordination compounds. Rotation is chosen from heavier towards lighter atoms in L-threoninate, and the straight arrow shows: "up", ↑, or "down", ↓, direction.

coordinated to the copper(II) atom in the basal plane. Bond length and angles in the basal plane (Cu–N bond lengths are in the range 1.971(2)–2.039(6) Å, and Cu–O lengths are in the range 1.899(16)–1.974(14) Å) correspond to those in similar compounds found in the literature [7, 44] (Table S3 in Supplementary information). Most of the Cu–$O_{water}$ apical bonds (2.181(4)–2.257(6) Å) are somewhat shorter than other apical Cu–O bonds ($d$(Cu–$O_{methanol}$) = 2.244(7)–2.347(3) Å; $d$(Cu–$O_{carboxylate}$) = 2.282(7)–2.338(6) Å and $d$(Cu–$O_{sulfate}$) = 2.382 (6) Å) (Table S3 in Supplementary information). The apical Cu–$N_{pyridine}$ bond (2.175 (9) Å) in **1f** is shorter than the apical Cu–O bonds (Table S3 in Supplementary information).

### 3.3.2. *Non-covalent interactions and structural isomerism*

All structures contain numerous potential hydrogen bond donors and acceptors, such as amino-, hydroxyl- and carboxylate groups of L-threoninate, solvent molecules, sulfate or hydrogensulfate ions, so most of the compounds contain complex hydrogen-bonded frameworks. Some hydrogen bond motifs are conserved in all eight compounds. At least one

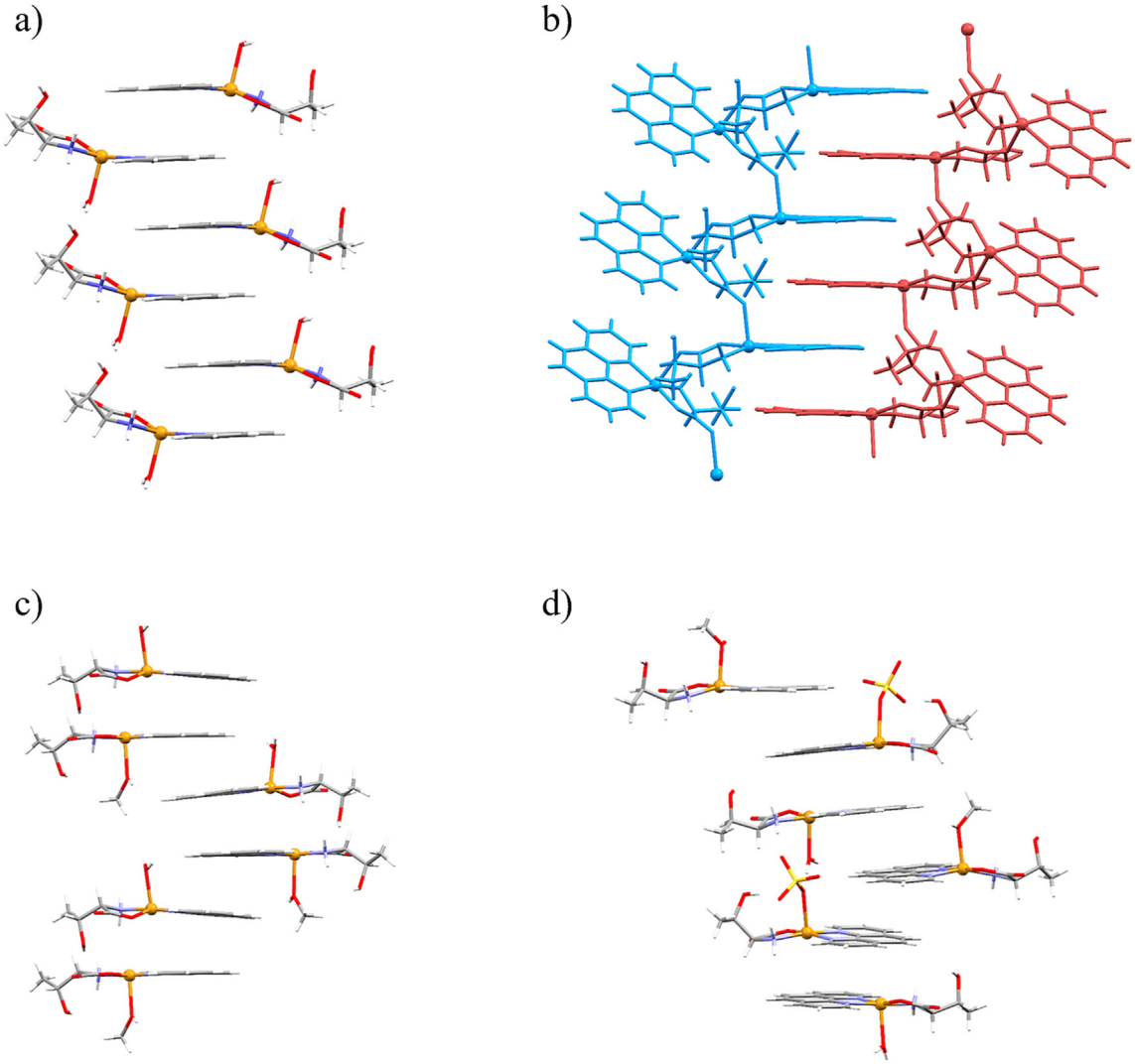


**Figure 4.** Different types of stacking of the complex species: a) alternating $\uparrow_{H2O}$ and $\downarrow_{H2O}$ complex cations in **1a•10$H_2O$**; b) interlocked polymeric chains in **1b•3.5$H_2O$**; c) $\uparrow_{H2O}$ and $\downarrow_{MeOH}$ complex cations dimers connected in zig-zag fashion in **1c•$H_2O$•2$CH_3OH$**; d) 1D pillars formed by stacking of all three complex species alternating in order $\uparrow_{MeOH}$ $\uparrow_{SO4}$ $\downarrow_{H2O}$ in **1e•$H_2O$•3$CH_3OH$**.

**Table 1.** Types of packing of crystallization solvent molecules and volume ratio of solvent molecules in all investigated compounds.

| Compound | Type of packing | $V$ (solvent)/$V$ (unit cell) |
|---|---|---|
| **1a•10H$_2$O** | 1D channels | 25.7% |
| **1a•4.3H$_2$O** | 1D channels and pockets | 12.1% |
| **1b•3.5H$_2$O** | pockets | 14.1% |
| **1c·4H$_2$O** | 1D channels and pockets | 11.3% |
| **1c•H$_2$O•2CH$_3$OH** | pockets | 11.2% |
| **1d•H$_2$O** | pockets | 5.2% |
| **1e•H$_2$O•3CH$_3$OH** | pockets | 14.1% |
| **1f** | / | 0% |

amino- and one hydroxyl group of L-threoninate ligand in each compound are involved in N–H···O$_{sulfate}$ and O–H···O$_{sulfate}$ hydrogen bonds, which act as a bridge between two adjacent complex species (in **1e•H$_2$O•3CH$_3$OH** one N–H···O$_{sulfate}$ and O–H···O$_{sulfate}$ hydrogen bond is intramolecular) (Table S4 and S5 in Supplementary information).

In **1e•H$_2$O•3CH$_3$OH** a rare hydrogen sulfate···sulfate hydrogen bond is found (Figure 2). In a CSD search in which close contacts of hydrogen sulfate and sulfate anions were defined as an intermolecular contact with H···O distance shorter than the sum of van der Waals radii, 298 data sets were found. In another search, the same query was defined but limited to the structures containing any transitional metal. 51 data sets were found, which is only 1.5% of all data sets found in CSD containing any transitional metal and sulfate ions. In **1e•H$_2$O•3CH$_3$OH** the sulfate ion is coordinated to the copper atom in one of the symmetrically independent complex species and acts as an acceptor for the hydrogen bond with the hydrogen sulfate ion ($d$(O–H···O) = 2.574 (8) Å; Fig. S4 in Supplementary information). S–O bond distances in the coordinated sulfate are in the range 1.463(7)–1.481(5) Å, and the unprotonated S–O groups of the hydrogen sulfate ion S–O bond distances are in the range 1.435(6)–1.472(7) Å. In the protonated S–O group, the S–O bond is significantly

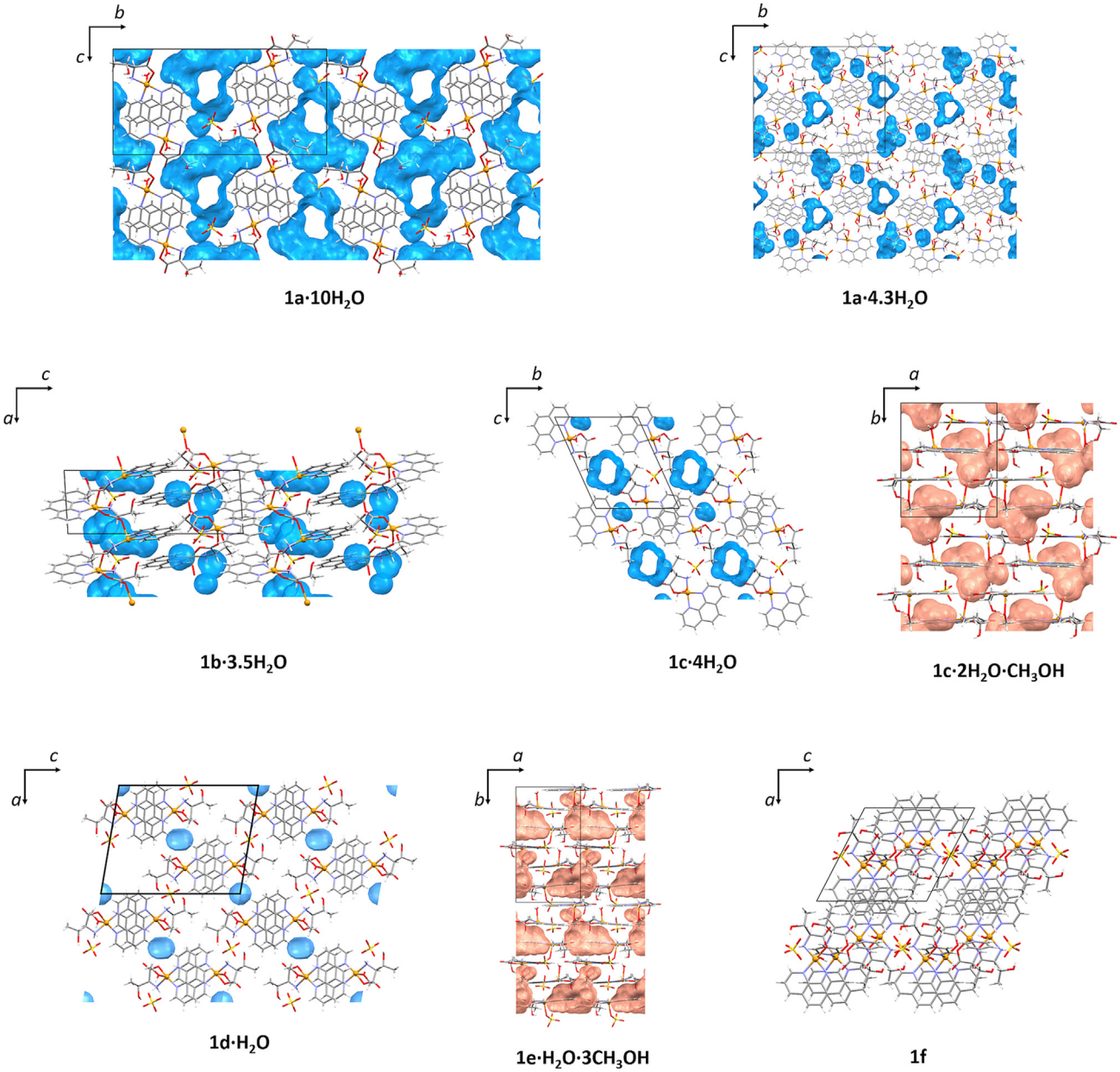


**Figure 5.** Crystal packing of all eight compounds: **1a•10H$_2$O**, **1a•4.3H$_2$O**, **1b•3.5H$_2$O**, **1c•2H$_2$O•CH$_3$OH**, **1c•4H$_2$O**, **1d•H$_2$O**, **1e·H$_2$O·3CH$_3$OH** and **1f**. Blue surfaces represent contact surface of water molecules, and orange surfaces represent contact surface of water and methanol molecules. Disordered water molecule in **1a•4.3H$_2$O** is not represented with contact surface.

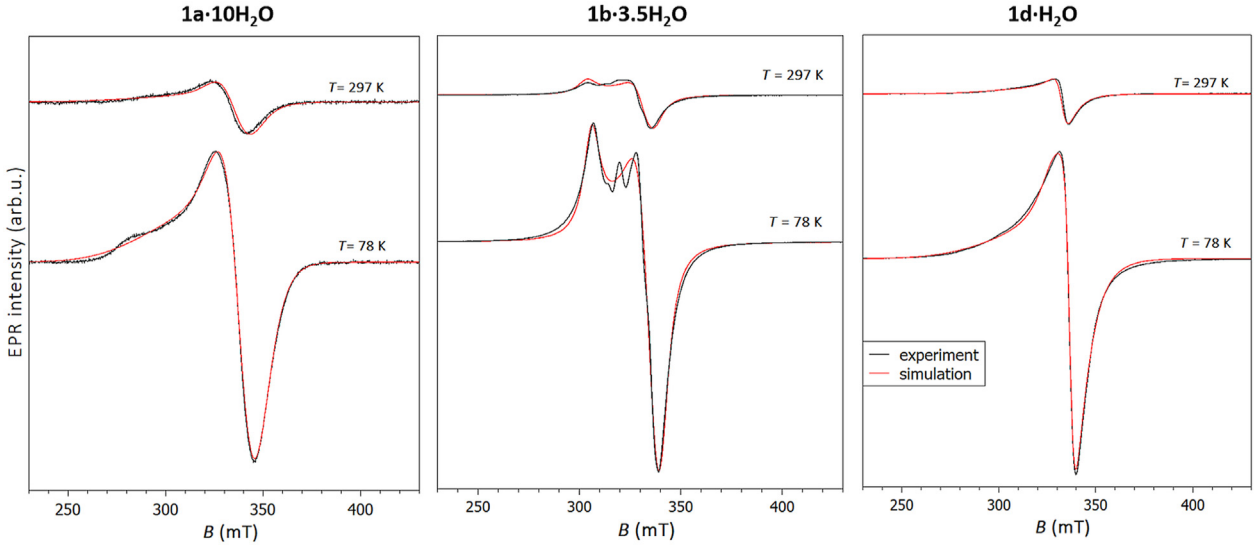


**Figure 6.** Experimental (black lines) and simulated (red lines) ESR spectra of polycrystalline samples of the investigated complexes **1a•10H$_2$O** (left), **1b•3.5H$_2$O** (middle) and **1d•H$_2$O** (right). The ESR intensities of the spectra at different temperatures are presented in the real ratios.

**Table 2.** The principal *g*-values obtained from the ESR spectral simulations, together with the parameter used for the simulations: $g_{strain}$ and linewidths $l_w$.

| Compound | $g = [g_x\ g_y\ g_z]$ | $g_{strain}$ | $l_w$ (mT) | $T$ (K) |
|---|---|---|---|---|
| **1a•10H$_2$O** | [2.05 2.05 2.30] | [0.08 0.13 0.44] | 0.23 | 78 |
| | | [0.10 0.09 0.52] | 0.23 | 297 |
| **1b•3.5H$_2$O** | [2.05 2.09 2.27] | [0.02 0.04 0.00] | 5.68 | 78 |
| | | [0.01 0.00 0.00] | 6.60 | 297 |
| **1d•H$_2$O** | [2.06 2.07 2.25] | [0.02 0.1 0.45] | 0.23 | 78 |
| | | [0.0 0.00 0.31] | 4.51 | 297 |

**Table 3.** *In vitro* cytotoxicity ($IC_{50}$ values[a]) of compound **1a•10H$_2$O**.

| Compound | $IC_{50}$/μmol L$^{-1}$ | |
|---|---|---|
| | HepG2 | THP1 |
| **1a•10H$_2$O** | 60.6 | 3.64 |
| staurosporine | 34.7 | 0.2 |

[a] Concentration that causes 50% inhibition of the cell growth.

longer with a distance of 1.568 (6) Å, which is in accordance with literature data [45, 46].

Due to asymmetrically coordinated copper in the basal plane, two optical isomers may be distinguished based on the position of the apically coordinated atom. "Up", ↑, and "down", ↓, positions of apically coordinated atom are defined using the right-hand rule shown in Figure 3.

All compounds contain both ↑ and ↓ isomers, however, since all structures are noncentrosymmetric, not all structures contain mixtures of those isomers. In **1a•10H$_2$O**, **1a•4.3H$_2$O**, **1b•3.5H$_2$O**, and **1d•H$_2$O** only one type of the apical ligand is present, and all those structures contain mixtures of ↑ and ↓ isomers. In **1c•2H$_2$O•CH$_3$OH**, **1c•4H$_2$O**, **1e•H$_2$O•3CH$_3$OH**, and **1f**, all complex cations with apically coordinated water are ↓ isomers, while complexes with apically coordinated methanol, pyridine and sulfate ions are all ↑ isomers.

1,10-phenanthroline ligands tend to form supramolecular 1D pillars through π-interactions, which are formed in all eight compounds. 1,10-phenanthroline ligands of the adjacent complexes within the supramolecular chain are almost coplanar in all compounds. Depending on the type of the ligands are coordinated in the apical position, different types of chains are formed. In compounds **1a·10H$_2$O**, **1a·4.3H$_2$O**, **1b·3.5H$_2$O**, **1c·4H$_2$O** and **1d·H$_2$O**, complex species are stacked through π-interactions with ↑ and ↓ complexes alternating so that ↑ complexes are on one side of the π-stacked chain, while ↓ complexes are on the other side of the chain (Figure 4a).

In **1b·3.5H$_2$O** polymeric chains are interlocked by π-interactions forming supramolecular 2D sheets (Figure 4b.). In **1c·H$_2$O·2CH$_3$OH** and **1f** ↑ and ↓ complex cations form sandwich-like dimers which are alternating in a zig-zag pattern (Figure 4c). Finally, **1e•H$_2$O•3CH$_3$OH** contains three different complex species, having apically coordinated water or methanol molecules or sulfate ions. In this compound 1D pillars are formed by stacking all three complex species alternating in order ↑$_{MeOH}$ ↑$_{SO4}$ ↓$_{H2O}$ (Figure 4d).

### 3.3.3. Crystallization solvent molecules

Specific structure of investigated copper(II) ternary complex species, with half of the complex being hydrophobic, and the other half hydrophilic, has a consequence that hydrophobic phenanthroline ligands are oriented towards the inner side of π-stacked 1D pillars, while the hydrophilic parts of the complex species are oriented towards the outside of 1D pillars. This feature of the complex species is probably the reason why so many different solvates may be formed from very similar synthetic conditions. Between the pillars, crystallization solvent molecules form either 1D infinite chains (**1a•10H$_2$O**), pockets and 1D chains (**1a•4.3H$_2$O**, **1c·4H$_2$O**) or pockets (**1b•3.5H$_2$O**, **1c•H$_2$O•2CH$_3$OH**, **1d•H$_2$O**, **1e•H$_2$O•3CH$_3$OH**), as shown in Table 1 and Figure 5. It seems that not only the type and number of crystallization solvent molecules but also the type of coordinated species in the apical position has an influence on the formation of 1D chains. In **1a•10H$_2$O** crystallization water molecules occupy 25% of the unit cell volume, and this is the only compound having only 1D chains. **1a•4.3H$_2$O**, **1b•3.5H$_2$O**, **1c·4H$_2$O**, **1c•H$_2$O•2CH$_3$OH** and **1e•H$_2$O•3CH$_3$OH** have comparable ratio of crystallization water molecules (Table 1), but only **1a•4.3H$_2$O** and **1c·4H$_2$O** form 1D chains, along with pockets, of water molecules.

Influence of the apically coordinated molecule on the formation of pockets or channels of solvent molecules is also observed in the crystal structure of **1f**. In this structure, one of the symmetrically independent complex cations has coordinated pyridine, while the other has a coordinated water molecule. Coordinated pyridine does not have a free acceptor or strong hydrogen bond donor atoms, and the structure does not contain crystallization solvent molecules.

### 3.4. ESR spectroscopy

Three polycrystalline ternary copper(II) complexes **1a•10H$_2$O**, **1b•3.5H$_2$O** and **1d•H$_2$O** were investigated by X-band electron spin resonance (ESR) spectroscopy. The representative spectra, obtained at room temperature (297 K) and liquid nitrogen temperature (78 K), are shown in Figure 6.

The spectral simulations were performed by EasySpin software [47] using the following form of the spin-Hamiltonian for copper (II) ions [48, 49]:

$$\mathbf{H} = \mu_B \, \mathbf{B} \cdot \mathbf{g} \cdot \mathbf{S} + \mathbf{S} \cdot \mathbf{A} \cdot \mathbf{I}. \quad (1)$$

In Eq. (1) $\mu_B$ is Bohr magneton, **g** is the **g**-tensor, **B** is the magnetic field, **S** and **I** are the electron and nuclear spin operator, respectively while hyperfine tensor **A** describes interaction between electron and nuclear spins. For all simulations, the second term in Eq. (1) was omitted because hyperfine interaction was not experimentally observed.

The spectra were simulated using the same values of **g**-tensor at both temperatures, allowing linewidth of assumed Lorentzian lineshape to change with temperature. The spin-Hamiltonian values, obtained from the simulations, are given in Table 2. Small variations in the local geometry of the Cu(II) coordination can cause distribution of $g_x$, $g_y$ and $g_z$-values around some average values [50]. This effect described by $\mathbf{g}_{strain}$ parameters is also considered in the simulations with the values presented in Table 2. The obtained *g*-values $g_x \approx g_y < g_z$ are expected for the elongated octahedral, square pyramidal or square planar copper geometry [51], and are in agreement with structurally determined distorted square pyramidal geometries in these compounds. Although all investigated complexes contain more than one copper(II) atom per unit cell, only one ESR line is observed in the powder spectra due to similar geometries and *g*-parameters. The distances between two nearest copper atoms are 6.584 Å and 6.389 Å, for **1a•10H$_2$O** and **1d•H$_2$O**, respectively, while **1b•3.5H$_2$O** is an one-dimensional zig-zag polymer with the distance between two nearest copper atoms of 5.487 Å. Therefore, the Cu–Cu distances are large enough to observe significant exchange interactions in these compounds. **1b•3.5H$_2$O** is unstable outside of solution and a sample was poorly grinded into powder, resulting in observation of additional crystalline peaks in the powder spectrum.

### 3.5. Cytotoxicity

The results of the cell viability assay with $IC_{50}$ values are presented in Table 3. **1a•10H$_2$O** showed substantial cytotoxic activity toward human hepatocellular carcinoma (HepG2) and acute monocytic leukaemia (THP-1) cell lines. Moreover, it exhibited somewhat lowered cytotoxicity against THP-1 cells. Similar ternary copper complexes, investigated by different research groups, showed that mode of their action against tumor cells was DNA cleavage via reactive oxygen species (ROS) generation, mitochondrical toxicity or direct interaction with DNA after their administration to tumor cells [13, 52, 53, 54, 55]. Quantitative structure-activity relationship (QSAR) studies on similar ternary copper compounds indicated that the presence of phenanthroline was necessary to preserve the antiproliferative activity and that the nature of the O,N coligand had a poor influence on biological activity [56]. We believe that the square pyramidal structure of compound **1a•10H$_2$O** with planar phenathroline ligand, L-Thr coligand and apically coordinated water molecule provides an optimal geometry for interaction with DNA strands through π-stacking interaction (phenathroline with DNA bases) and hydrogen bonds (L-Thr and apically coordinated water molecule with DNA bases) [3, 57]. However, comprehensive research on mode of action of **1a•10H2O** is needed to compare antitumor activities on different cell lines.

## 4. Conclusions

Eight new ternary copper(II) coordination compounds with 1,10-phenanthroline and L-threonine were obtained by solution-based syntheses (**1a•10H$_2$O**, **1a•4.3H$_2$O**, **1b•3.5H$_2$O**, **1c•2H$_2$O•CH$_3$OH**, **1c•4H$_2$O**, **1d•H$_2$O**, **1e·H$_2$O·3CH$_3$OH**, **1f**) and three of them also by mechanochemical syntheses (**1a•10H$_2$O**, **1c•2H$_2$O•CH$_3$OH** and **1d•H$_2$O**). We have found that different synthetic approach can control porous and non-porous structures in a controlled manner. It was shown that small differences in water content in synthetic mixtures (and possibly atmospheric conditions) have a high influence on the final product in both solution-based and mechanochemical syntheses, so in some cases two or three different products were obtained. All compounds consist of three different types of complex unit (named type 1, type2 and type 3). In all complex units the copper(II) ion is pentacoordinated by a L-threoninate and a phenanthroline ligand in the equatorial plane, and apically by a solvent molecule (either a water, methanol or pyridine molecule) in the type 1 complex cation, by sulphate in the type 2 complex anion and by carboxylate of a neighbouring complex cation in the type 3 complex unit. Two types of diastereomers are found for the complex unit regarding the position of the apically coordinated species in relation to the chiral L-threoninato ligand (named up and down). All compounds except **1f** are different solvates with solvent molecules situated either in the endless 1D channels and/or pockets. In all crystal structures of the solvates, the complex units, sulfate or hydrogensulfate anions and solvent molecules are linked by hydrogen bonds and π-interactions into 3D supramolecular frameworks. Compounds described in this study form some predictive intermolecular interactions such as π-interactions or certain hydrogen bond motifs (N–H···O$_{sulfate}$ and O–H···O$_{sulfate}$). Knowledge of intermolecular interactions might help in the design of new compounds for potential drug design and/or functional material in the separation industry. ESR analysis of the different types of compounds showed agreement of the obtained *g*-values of the copper unpaired electron with the elongated square-pyramidal geometries of copper ions. Compound **1a•10H$_2$O** showed substantial cytotoxic activity toward human HepG2 and THP-1 cell lines. Found biologycal activity provides an incentive to further study in different tumor cells.

## Associated content

Supporting Information. The supporting material contains crystallographic data, ORTEP drawings of crystal structures, selected hydrogen bond distances and angles, powder X-ray diffraction patterns.

## Declarations

### Author contribution statement

Darko Vušak, Jurica Jurec: Conceived and designed the experiments; Performed the experiments; Analyzed and interpreted the data; Wrote the paper.

Katarina Ležaić: Performed the experiments; Analyzed and interpreted the data.

Dijana Žilić, Biserka Prugovečki: Conceived and designed the experiments; Performed the experiments; Analyzed and interpreted the data; Contributed reagents, materials, analysis tools or data; Wrote the paper.

### Funding statement

This work was supported by the Croatian Government and the European Union through the European Regional Development Fund-Competitiveness and Cohesion Operational Programme (Grant KK.01.1.1.02.0016), and The Croatian Science Foundation (grant no IP-2018-01-3168).

### Data availability statement

Data included in article/supplementary material/referenced in article.

## Declaration of interests statement

The authors declare no conflict of interest.

## Additional information

Supplementary content related to this article has been published online at https://doi.org/10.1016/j.heliyon.2022.e09556.

## References


[1] M.C. Linder, Biochemistry of Copper, 10, Springer Science & Business Media, 2013.
[2] M. Yodoshi, M. Odoko, N. Okabe, Structures and DNA-binding and cleavage properties of ternary copper(II) complexes of Glycine with phenanthroline, bipyridine, and bipyridylamine, Chem. Pharm. Bull. 55 (6) (2007) 853–860.
[3] J.C. García-Ramos, R. Galindo-Murillo, A. Tovar-Tovar, A.L. Alonso-Saenz, V. Gómez-Vidales, M. Flores-Álamo, L. Ortiz-Frade, F. Cortes-Guzmán, R. Moreno-Esparza, A. Campero, L. Ruiz-Azuara, The π-back-bonding modulation and its impact in the electronic properties of CuII antineoplastic compounds: an experimental and theoretical study, Chem. Eur J. 20 (2014) 13730–13741.
[4] H.-L. Seng, W.-S. Wang, S.-M. Kong, H.-K.A. Ong, Y.-F. Win, R.N.Z.R.A. Rahman, M. Chikira, W.-F. Leong, M. Ahmad, A.-S.-B. Khoo, C.-H. Ng, Biological and cytoselective anticancer properties of copper(II)-polypyridyl complexes modulated by auxiliary methylated glycine ligand, Biometals 25 (2012) 1061–1081.
[5] D. Vušak, B. Prugovečki, D. Milić, M. Marković, I. Petković, M. Kralj, D. Matković-Čalogović, Synthesis and crystal structure of solvated complexes of copper (II) with serine and phenanthroline and their solid-state-to-solid-state transformation into one stable solvate, Cryst. Growth Des. 17 (2017) 6049–6061.
[6] P.Y. Ng, S.M. Chye, Y.L. Tiong, C.W. Chan, K.W. Tan, I.H. Ooi, C.H. Ng, Enantiomeric pairs of copper(II) polypyridyl-alanine complex salts: anticancer studies, Transit. Met. Chem. 43 (2018) 479–496.
[7] S. Zhang, Y. Zhu, C. Tu, H. Wei, Z. Yang, L. Lin, J. Ding, J. Zhang, Z. Guo, A novel cytotoxic ternary copper(II) complex of 1,10-phenanthroline and L-threonine with DNA nuclease activity, J. Inorg. Biochem. 98 (2004) 2099–2106.
[8] C.-X. Ren, M. Ji, Q.-X. Yao, L.-X. Cai, B. Tan, J. Zhang, Targeted functionalization of porous materials for separation of alcohol/water mixtures by modular assembly, Chem. Eur. J. 20 (2014) 14846–14852.
[9] B.-Y. Lou, F.-L. Jiang, B.-L. Wu, D.-Q. Yuan, M.-C. Hong, From helical array to porous architecture: exploring the use of side chains of amino acids to engineer 1D infinite coordination polymeric chain into porous frameworks, Cryst. Growth Des. 6 (4) (2006) 989–993.
[10] B.-Y. Lou, R.-H. Wang, D.-Q. Yuan, B.-L. Wu, F.-L. Jiang, M.-C. Hong, Two homochiral 3D supramolecular architectures assembled from 4,4'-bipyridine-bridged copper(II) amino acid helical chains, Inorg. Chem. Commun. 8 (2005) 971–974.
[11] L. Ruiz-Azuara, Copper Amino Acidate Diimine Nitrate Compounds and Their Methyl Derivatives and a Process for Preparing Them, U.S. Patent 5, 1996, p. 576, 326, November 19.
[12] L. Ruiz-Azuara, Process to obtain new mixed copper aminoacidate complexes from phenylatephenanthroline to be used as anticancerigenic agents, U.S. Patent RE 35 (1997) 458. Febrary 18.
[13] L. Ruiz-Azuara, M.E. Bravo-Gómez, Copper compounds in cancer Chemotherapy, Curr. Med. Chem. 17 (2010) 3606–3615.
[14] C.R. Groom, I.J. Bruno, M.P. Lightfoot, S.C. Ward, The Cambridge structural database, Acta Crystallogr. B72 (2016) 171–179.
[15] M.L. Low, C.W. Chan, P.Y. Ng, I.H. Ooi, M.J. Maah, S.M. Chye, K.W. Tan, S.W. Ng, Ternary and binary copper(II) complexes: synthesis, characterization, ROS-inductive, proteasome inhibitory, and anticancer properties, J. Coord. Chem. 70 (2) (2017) 223–241.
[16] W.C. Zhang, X. Tang, X. Lu, One-dimensional chiral copper(II) complexes with novel nano-structures and superior antitumor activity, J. Inorg. Biochem. 156 (2016) 105–112.
[17] L. Antolini, L.P. Battaglia, A. Bonamartini Corradi, G. Marcotrigiano, L. Menabue, G.C. Pellacani, M. Saladini, M. Sola, Tridentate facially coordinated L-aspartate ion complexation with the copper(II) ion: spectroscopic and structural properties of aqua(L-aspartato)(1,10-phenanthroline)copper(II) tetrahydrate, Inorg. Chem. 25 (1986) 2901–2904.
[18] L.P. Battaglia, A. Bonamartini Corradi, L. Antolini, G. Marcotrigiano, L. Menabue, G.C. Pellacani, Coordination behavior of L-aspartic acid: ternary nickel(II) complexes with imidazoles. Crystal and molecular structure of (L-aspartate) tris(imidazole)nickel(II), J. Am. Chem. Soc. 104 (1982) 2407–2411.
[19] L. Antolini, G. Marcotrigiano, L. Menabue, G.C. Pellacani, Coordination behavior of L-aspartic acid: thermal, spectroscopic, magnetic, and structural properties of aqua(L-aspartato)(2,2'-bipyridine)copper(II) trihydrate, Inorg. Chem. 22 (1983) 141–145.
[20] A. Wojciechowska, T. Rojek, M. Malik−Gajewska, M. Jerzykiewicz, R. Wysokiński, A. Gągor, P. Rytlewski, Z. Staszak, M. Duczmal, Crystal and molecular structure stabilized by weak interaction in unique 3,5-diiodo-L-tyrosinato copper(II) complex – synthesis, experimental and theoretical studies, Mater. Sci. Eng. B 262 (2020), 114723.
[21] C.-C. Su, T.-Y. Tai, S.-P. Wu, S.-L. Wang, F.-L. Liao, Spectroscopic and electronic properties of mixed ligand aminoacidatocopper(II) complexes, Polyhedron 18 (1999) 2361–2368.
[22] D. İnci, R. Aydın, H. Huriyet, Y. Zorlu, N. Çinkılıç, Newly synthesized Cu(II) pyrazino[2,3-f][1,10]phenanthroline complexes as potential anticancer candidates, Appl. Organomet. Chem. 32 (2018) e4309.
[23] D. İnci, R. Aydın, T. Sevgi, Y. Zorlu, E. Demirkan, Synthesis, crystal structure, stability studies, DNA/albumin interactions, and antimicrobial activities of two Cu(II) complexes with amino acids and 5-nitro-1,10-phenanthroline, J. Coord. Chem. 70 (2017) 512–543.
[24] R.-T. Chen, Q.-Y. Zhang, Y.-J. Li, Kinetics and mechanisms of ternary complex formation between (5-X-1,10-phenanthroline)copper(II) and threonine, Acta Chim. Sin. 47 (1989) 342–348.
[25] J.E. Letter, J.E. Bauman, A thermodynamic study of the complexation reactions for a series of amino acids related to serine with copper(II) and nickel(II), J. Am. Chem. Soc. 92 (1970) 437–442.
[26] L. Gasque, R. Moreno-Esparza, L. Ruiz-Ramírez, Stability of ternary copper and nickel complexes with 1,10-phenanthroline, J. Inorg. Biochem. 48 (1992) 121–127.
[27] D. İnci, R. Aydın, Stabilities of the ternary complexes of copper(II) with substituted 1,10-phenanthrolines and some amino acids in aqueous solution, J. Solut. Chem. 43 (2014) 711–726.
[28] N. Türkel, Çiğdem Şahin, Stability of binary and ternary copper(II) complexes with 1,10-phenanthroline, 2,2'-bipyridyl and some $\alpha$-amino acids in aqueous medium, Chem. Pharm. Bull. 57 (2009) 694–699.
[29] D. Vušak, B. Prugovečki, D. Matković- Čalogović, Synthesis, structure and chemical properties of copper(II) complexes with 2,2'-bipyridine and L-serine: porous materials and polymorphism, Acta Crystallogr. A74 (2018) E337.
[30] D. Vušak, K. Ležaić, B. Prugovečki, D. Matković-Čalogović, Coordination polymers and solvatomorphs-copper complexes with amino acids and 2,2'-bipyridine, Acta Crystallogr. A74 (2019) E530.
[31] B. Prugovečki, D. Vušak, K. Ležaić, M. Jurković, Ternary coordination compounds of copper with amino acids and 1,10-phenanthroline–structural insight and biological activity, Acta Crystallogr. A77 (2021) C975.
[32] G. Brauer (Ed.), Handbook of Preparative Inorganic Chemistry, second ed., Academic Press, New York, 1965.
[33] A.N. Agte, N.S. Golynko, Production of chemically-pure $Cu(OH)_2$ and $Cu(OAc)_2$. Determination of the solubility of $Cu(OAc)_2$ in water. Production of technical $Cu(OAc)_2$, Trudy Leningr. Khim.-Tekh. Inst. 8 (1940) 140–149.
[34] T. Degen, M. Sadki, E. Bron, U. König i G. Nénert, The HighScore suite, Powder Diffr. 29 (2014) S13–S18.
[35] E. Melnic, E.B. Coropceanu, O.V. Kulikova, A.V. Siminel, D. Anderson, H.J. Rivera-Jacquez, A.E. Masunov, M.S. Fonari, V. Ch. Kravtsov, Robust packing patterns and luminescence quenching in mononuclear $[Cu(II)(phen)_2]$ sulfates, J. Phys. Chem. C 118 (2014) 30087–30100.
[36] J.-L. Do i T. Friščić, Mechanochemistry: a force of synthesis, ACS Cent. Sci. 3 (2017) 13–19.
[37] CrysAlisPRO Software System, Oxford Diffraction / Agilent Technologies UK Ltd, Yarnton, England, 2018.
[38] G.M. Sheldrick, A short history of SHELX, Acta Crystallogr. Sect. A Found. Crystallogr. 64 (2008) 112–122.
[39] G.M. Sheldrick, Crystal structure refinement with SHELXL, Acta Crystallogr. Sect. C Struct. Chem. 71 (2015) 3–8.
[40] G.M. Sheldrick, SHELXT – Integrated space-group and crystalstructure determination, Acta Crystallogr. Sect. A Found. Adv. 71 (2015) 3–8.
[41] C.F. Macrae, I.J. Bruno, J.A. Chisholm, P.R. Edgington, P. McCabe, E. Pidcock, L. Rodriguez-Monge, R. Taylor, J. van de Streek i, P.A. Wood, Mercury CSD 2.0 – new features for thevisualization and investigation of crystal structures, J. Appl. Crystallogr. 41 (2008) 466–470.
[42] A.L. Spek, Structure validation in chemical crystallography, Acta Crystallogr. Sect. D Biol. Crystallogr. 65 (2009) 148–155.
[43] T. Mosmann, Rapid colorimetric assay for cellular growth and survival: application to proliferation and cytotoxicity assays, J. Immunol. Methods 65 (1–2) (1983) 55–63.
[44] Y.-H. Tav, S.-G. Teoh, K.-L. Sek, W.-S. Loh, H.-K. Fun, Aqua(1,10-phenanthroline-$\kappa^2N,N'$)(DL-threoninato-$\kappa^2N,O^1$)copper(II) chloride dihydrate, Acta Crystallogr. E 66 (2010) m595–m596.
[45] G.K. Kole, G.K. Tan, J.J. Vittal, Anion-controlled stereoselective synthesis of Cyclobutane derivatives by solid-state [2 + 2] Cycloaddition reaction of the salts of trans-3-(4-Pyridyl) acrylic acid, Org. Lett. 12 (1) (2010) 128–131.
[46] M.-L. Tong, S.-L. Zheng, X.-M. Chen, Self-assembly of two- and three-dimensional coordination networks with hexamethylenetetramine and different silver(I) salts, Chem. Eur J. 6 (No. 20) (2000) 3729–3738.
[47] S. Stoll, A. Schweiger, EasySpin, a comprehensive software package for spectral simulation and analysis in EPR, J. Magn. Reson. 178 (2006) 42.
[48] O. Kahn, Molecular Magnetism, Wiley-VCH Inc., 1993.
[49] A. Carrington, MAD, Introduction to Magnetic Resonance, Harper & Row, New York, 1967.
[50] B. Szymańska, D. Skrzypek, D. Kovala-Demertzi, M. Staninska, M.A. Demertzis, Synthesis and spectroscopic study of copper(II) and manganese(II) complexes with pipemidic acid, Spectrochim. Acta 63 (2006) 518–523.
[51] E. Garribba, G. Micera, The determination of the geometry of Cu(II) complexes: an EPR spectroscopy experiment, J. Chem. Educ. 83 (2006) 1229–1232.
[52] C. Santini, M. Pellei, V. Gandin, M. Porchia, F. Tisato, C. Marzano, Advances in copper complexes as anticancer agents, Chem. Rev. 114 (2014) 815–862.
[53] A.I. Valencia-Cruz, L.I. Uribe-Figueroa, R. Galindo-Murillo, K.B. López, A.G. Gutiérrez, A. Vázquez-Aguirre, L. Ruiz-Azuara, E. Hernández-Lemus, C. Mejía C, Whole genome gene expression analysis reveals casiopeina-induced apoptosis pathways, PLoS One 8 (1) (2013), e54664.

[54] A.G. Gutiérrez, A. Vázquez-Aguirre a, J.C. García-Ramos, M. Flores-Alamo, E. Hernández-Lemus, L. Ruiz-Azuara, C. Mejía, Copper(II) mixed chelate compounds induce apoptosis through reactive oxygen species in neuroblastoma cell line CHP-212, J. Inorg. Biochem. 126 (2013) 17–25.

[55] L. Becco, J.C. García-Ramos, L. Ruiz Azuara, D. Gambino, B. Garat, Analysis of the DNA interaction of copper compounds belonging to the Casiopeínas® antitumoral series, Biol. Trace Elem. Res. 161 (2014) 210–215.

[56] M.E. Bravo-Gomez, J.C. Garcia-Ramos, I. Gracia-Mora, L.J. Ruiz-Azuara, Antiproliferative activity and QSAR study of copper(II) mixed chelate [Cu(N–N)(acetylacetonato)]$NO_3$ and [Cu(N–N)(glycinato)]$NO_3$ complexes,(Casiopeínas®) Inorg, Biochemistry 103 (2009) 299–309.

[57] R. Galindo-Murillo, J. Hernandez-Lima, M. Gonzalez-Rendon, F. Cortes-Guzman, L. Ruiz-Azuara, R. Moreno-Esparza, π-Stacking between Casiopeínas® and DNA bases, Phys. Chem. Chem. Phys. 13 (2011) 14510–14515.